Diagnosis of meningioma by time-resolved fluorescence spectroscopy

Pramod V. Butte
University of Southern California
Department of Biomedical Engineering
Los Angeles, California 90089
and
Cedars-Sinai Medical Center
Biophotonic Research and Technology Development
Los Angeles, California 90048

Brian K. Pikul
Cedars-Sinai Medical Center
Maxine-Dunitz Neurosurgical Institute
Los Angeles, California 90048

Aviv Hever
Cedars-Sinai Medical Center
Department of Pathology
Los Angeles, California 90048

William H. Yong
Cedars-Sinai Medical Center
Department of Pathology
Los Angeles, California 90048
and
University of California at Los Angeles
David Geffen School of Medicine
Los Angeles, California 90095

Keith L. Black
Cedars-Sinai Medical Center
Maxine-Dunitz Neurosurgical Institute
Los Angeles, California 90048

Laura Marcu
Cedars-Sinai Medical Center
Biophotonics Research and Technology Development
Los Angeles, California 90048

Abstract. We investigate the use of time-resolved laser-induced fluorescence spectroscopy (TR-LIFS) as an adjunctive tool for the intraoperative rapid evaluation of tumor specimens and delineation of tumor from surrounding normal tissue. Tissue autofluorescence is induced with a pulsed nitrogen laser (337 nm, 1.2 ns) and the intensity decay profiles are recorded in the 370 to 500 nm spectral range with a fast digitizer (0.2 ns resolution). Experiments are conducted on excised specimens (meningioma, dura mater, cerebral cortex) from 26 patients (97 sites). Spectral intensities and time-dependent parameters derived from the time-resolved spectra of each site are used for tissue characterization. A linear discriminant analysis algorithm is used for tissue classification. Our results reveal that meningioma is characterized by unique fluorescence characteristics that enable discrimination of tumor from normal tissue with high sensitivity (>89%) and specificity (100%). The accuracy of classification is found to increase (92.8% cases in the training set and 91.8% in the cross-validated set correctly classified) when parameters from both the spectral and the time domain are used for discrimination. Our findings establish the feasibility of using TR-LIFS as a tool for the identification of meningiomas and enables further development of real-time diagnostic tools for analyzing surgical tissue specimens of meningioma or other brain tumors.
 [DOI: 10.1117/1.2141624]

Keywords: meningioma; fluorescence spectroscopy; optical diagnostic; brain tumor diagnostic.

Paper 04243RR received Dec. 8, 2004; revised manuscript received Aug. 10, 2005; accepted for publication Aug. 19, 2005; published online Dec. 27, 2005.

1 Introduction

Meningiomas are slow growing lesions accounting for 15 to 20% of primary brain tumors. Surgical resection is the mainstay of treatment for meningiomas causing symptoms.[1–3] The extent of tumor resection directly correlates with prevention of recurrence. Intraoperative biopsy specimens are routinely removed by the neurosurgeon from the main tumor mass and possibly one to several dural margins. Neuropathologic evaluation for rapid intraoperative preliminary diagnosis is often requested. The standard intraoperative tissue specimen neuropathologic evaluation has been the "frozen section." This process of freezing the tissue, slicing the frozen specimen with a microtome, and staining/analysis can, at a minimum, take 15 to 25 min. Multiple intraoperative "frozen section" specimen requests can lead to lengthy increases in operative time, as well as a taxing increase in workload for the surgical pathologist. Certain intracranial characteristics of meningiomas, moreover, can increase the difficulty of achieving a complete surgical resection. The "en plaque" variety and petroclival location of meningiomas are examples of meningiomas that often present difficulty in excising dura involved with tumor. In addition, some meningiomas can invade the subjacent brain parenchyma, usually the cerebral cortex. Although conventional imaging techniques such as magnetic resonance imaging (MRI) and computed tomography (CT) can guide the surgery, each tumor's intraoperative appearance dictates the ease

Address all correspondence to Laura Marcu, University of California at Davis, Department of Biomedical Engineering, Davis, California 95616. E-mail: lmarcu@ucdavis.edu

1083-3668/2005/10(6)/064026/9/$22.00 © 2005 SPIE

with which a surgeon will accomplish complete tumor excision. Adjunctive instrumentation may provide additional benefit in achieving the goal of complete tumor resection. Time-resolved laser-induced fluorescence spectroscopy (TR-LIFS) represents a promising technique for identifying tumor in real time and may become an intraoperative adjunct for neuropathologic analysis and completeness of surgical tumor resections.

Laser-induced fluorescence spectroscopy (LIFS) is a useful tool for characterization of biological tissues and offers potential for *in vivo* diagnosis of diseased tissues and the optimization of therapeutic interventions.[4] The presence of intrinsic fluorophores such as amino acids (tyrosine, tryptophan), structural proteins (elastin, collagen), and enzyme cofactors (nicotinamide adenine dinucleotide, flavins) in human tissue offer the potential to probe biochemical, morphological, and physiological changes occurring in diseased tissues. The various alterations of these tissue fluorophores can be correlated by analyzing the changes of the relative contribution of each fluorescent constituent to the overall fluorescence emission. Either steady state[4–7] or time-resolved[8,9] fluorescence spectroscopy techniques can be used to measure or monitor these changes. Time-resolved measurement resolves fluorescence intensity decay in terms of lifetimes, and thus provides additional information than is available from the steady state measurement.[10,11]

Earlier work has demonstrated that LIFS of endogenous fluorophores (autofluorescence) can be used as a tool for diagnosis of neoplasms.[4,12–14] Several types of brain tumors have been investigated, both *in vivo* and *ex vivo*, using this technique. These include studies of glioblastoma[4,6,7,9,13] astrocytoma,[6] oligodendroglioma,[6] and metastatic carcinoma.[6] For example, combining fluorescence (excitation 337 nm) with diffuse reflectance spectroscopy at multiple excitation wavelengths[6] or using microspectrofluorometric measurements at a few excitation wavelengths,[13] it has been shown that brain tumors can be distinguished from normal brain tissue with good sensitivity and specificity. Our group has also reported results on the time-resolved fluorescence of glioblastoma.[9,15] However, to the best of our knowledge, no study has investigated the fluorescence emission of meningiomas and the potential of fluorescence spectroscopy for discrimination of meningiomas from the surrounding normal tissue.

In this study, we investigated the use of TR-LIFS technique as a diagnostic tool for intraoperative evaluation of meningioma tumor specimens (*ex vivo*) and delineation of tumor from surrounding normal tissue. Using an instrumental apparatus that enables simultaneous recording of both time-integrated (spectra) and time-resolved fluorescence, this study intends to (1) determine the spectrum- and time-dependent autofluorescence emission characteristics of human samples of meningioma, dura mater, and normal cortex using an ultraviolet laser (337 nm) as an excitation light source; (2) identify the main autofluorescence features that provide means of discrimination between tumor and surrounding normal tissue; and (3) determine the effectiveness of the fluorescence spectroscopy for recognition of the diseased tissue.

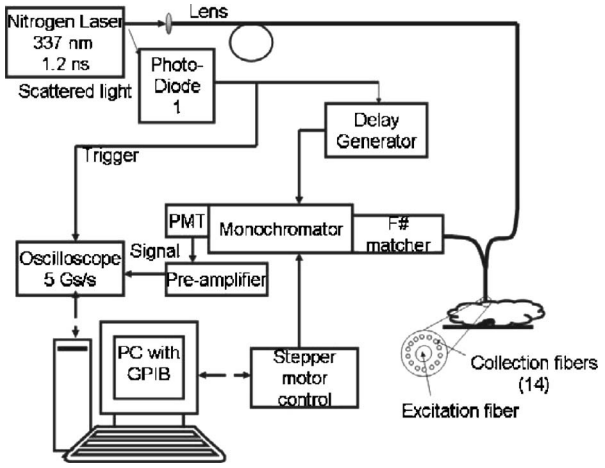

Fig. 1 Schematic of the instrumental setup for time-resolved fluorescence spectroscopy. (GPIB: General Purpose Interface Bus).

2 Methods

2.1 *Samples*

The study was conducted on tissue specimens from patients undergoing brain tumor surgery and histopathologically diagnosed as meningioma (total of 22 patients with various types of meningiomas: 8 transitional, 11 meningothelial, 1 psammomatous, 2 microcystic) and adjacent normal dura (4 patients). Samples of normal gray matter were obtained from 4 patients undergoing surgery for en-bloc resection of glioma brain tumor underlying cortex. The study was carried out with approval of the Cedars-Sinai Institutional Review Board. After excision, the specimens were kept in a sealed container and transported from the operating room to the spectroscopy laboratory. The spectroscopic investigations were performed within 30 to 120 min after excision. During the experimental procedure the samples were kept in a glass petri dish and soaked using 1 to 2 drops of saline to avoid drying of the tissue. Multiple distinct sites (total: 97) on the tissue were selected for spectroscopic investigation. After the completion of the spectroscopic procedure, the selected sites were marked using a dye and fixed in 10% buffered formalin, and then sent for histopathological studies. From each sample, transversely oriented sections (4 mm thick) were then cut from the marked areas. The tissues were embedded in paraffin and stained with hematoxylin-eosin (H&E). The histological sections were evaluated by light microscopy.

2.2 *Instrumentation*

The tissue samples were spectroscopically investigated with a prototype time-domain TR-LIFS apparatus (Fig. 1) similar to that used in previous studies.[8,9] A pulsed nitrogen laser (EG&G, model 2100; 337 nm, 1.2 ns, 10 Hz) was used as excitation light source. The output of the light source was delivered to the tissue by a custom-made bifurcated probe, which consists of a central excitation fiber (600 μm, numerical aperture 0.11) surrounded by a collection ring of 14 fibers (200 μm, numerical aperture 0.22). The collection fibers are beveled at a 10° angle in order to improve light excitation-collection overlap for small tissue to probe distances.[16] The pulse width measured at the tip of the fiber was 2.0 ns full

width at half maximum. The collected fluorescence emission was focused into a scanning monochromator (ORIEL, model 77200) using an *F#* matcher (ORIEL, model 77529), and detected by a gated multichannel plate photomultiplier tube (MCP-PMT; Hamamatsu, model R2024U, rise time: 0.3 ns) placed at the monochromator exit slit. The photomultiplier tube was gated using a high voltage gate (EG&G, ORTEC; 1 GHz). The photomultiplier output and the entire fluorescent pulse from a single excitation laser pulse was directed to a digital oscilloscope (Tektronics, model TDS 680C, sampling frequency: 5 Gsamples/s, bandwidth: 1 GHz) through a fast 1-GHz preamplifier (EG&G, ORTEC model 9306). The gating of the PMT was achieved using an optical switch triggered by laser pulse. To eliminate the scattering of the reflected excitation laser by the sample, a 360-nm long-pass filter was placed at the entrance slit of the monochromator and a 345-nm long-pass filter was placed in front of the PMT. A personal computer was used to control data acquisition, data transfer from oscilloscope, and monochromator wavelength scanning.

2.3 *Experimental Procedure*

The fiber optic probe was placed 3 mm above the tissue specimen to optimize the probe light collection efficiency, as previously reported.[16] Time-resolved emission of each sample was recorded in the 370 to 500 nm spectral range and scanned at 5 nm intervals. Five consecutive measurements of the fluorescence pulse emission at 390 and 460 nm are performed to assess the reproducibility of the fluorescence lifetime measurement. The energy output of the laser (at the tip of the fiber) for sample excitation was adjusted to 3.0 μJ/pulse.

2.4 *Data Analysis*

2.4.1 *Spectroscopic data processing*

The conventional spectral emission or time-integrated fluorescence spectrum was computed from the measured fluorescence pulses by integrating each pulse as a function of time for each investigated wavelength. The constructed fluorescence spectra was corrected for background noise and nonuniform instrumental system response, and then normalized by dividing the fluorescence intensity at each emission wavelength by the peak fluorescence intensity. The reconstructed spectrum was characterized by discrete intensity values (I_λ) that describe the variation of fluorescence intensity as a function of wavelength.

The time-resolved fluorescence spectrum or the fluorescence impulse response function (FIRF) was constructed by numerical deconvolution of the measured laser pulse from the measured fluorescence pulse at each wavelength across the spectrum. The deconvolution was based on the Laguerre expansion of kernels technique,[8,17] using five Laguerre functions. Deconvolution based on this technique separates the computation of the FIRF from the modeling of the fluorescent system, and therefore facilitates an unconstrained interpretation of time-resolved data from tissue. The dynamic of the fluorescence decay was characterized by two time-dependent parameters: the average lifetime τ_λ, estimated as the interpolated time at which the FIRF decays to $1/e$ of its maximum value, and the time-decay to 10%, $\tau_{\lambda:10\%}$, estimated as the interpolated time at which the FIRF decays to 10% of the maximum value. All computations were performed using the software package MATLAB® (Mathworks Inc.).

2.4.2 *Statistical analysis*

To compare the different tissue types based on their fluorescence emission characteristics multiple spectroscopic parameters were derived from the results: the ratio between the various fluorescence intensities (I_{440}/I_{370}, I_{450}/I_{370}, I_{460}/I_{370}, I_{470}/I_{370}, I_{480}/I_{370}, I_{390}/I_{440}, I_{460}/I_{390}), the time-dependent parameters near the peak observed at 390 nm (τ_{370}, τ_{380}, τ_{390}, $\tau_{370:10}$, $\tau_{380:10}$, $\tau_{390:10}$), and the time-dependent parameters near the peak observed at 460 nm ($\tau_{460:10}$,$\tau_{470:10}$, $\tau_{480:10}$). Statistical analysis was based on one-way analysis of variance (ANOVA) applied to these spectroscopic parameters. The level of significance used was ($P<0.05$).

2.4.3 *Classification*

A stepwise linear discriminant analysis was employed to determine the combination of predictor variables that accounts for most of the differences in the average profiles of the three tissue groups (meningioma, normal dura, and normal cortex), and to generate a classification model (discriminant functions) for samples classification. The discriminant function analysis not only provides an effective means for classifying spectroscopic data of unknown origin, but also is appropriate when the number of samples is small.[18] The spectral intensities used as input for the discriminant analysis were chosen based on the observed emission peaks at 390 and 460 nm of wavelength. To account for the breadth of emission, the intensity values around peak emission were also selected. This includes intensity values at 370 and 380 nm; and intensity values at 440, 450, 470, and 480 nm, respectively. The second consideration while deriving the parameters from the spectra was given to the fact that emission spectrum was normalized to the highest peak emission value. While the peak emission of meningioma and normal dura matter was at 390 nm, the peak emission of normal cortex was found at about 460 nm. This is likely to introduce errors when comparing spectra normalized with two different values. To avoid such errors caused by distinct normalization values and to compare the shapes of the spectrum independent of normalization values, we chose as parameters the ratios between normalized intensity at wavelengths close to peak emission and wavelengths at the two ends of the measured spectrum (I_λ/I_{370} and I_λ/I_{500}). Another set of parameters derived from the spectral data were the intensity ratios between the two observed peaks at 390 and 460 nm of wavelengths. Using the preceding criterion, the spectral parameters chosen were as follows: I_{440}/I_{370}, I_{450}/I_{370}, I_{460}/I_{370}, I_{470}/I_{370}, I_{480}/I_{370}, I_{390}/I_{370}, I_{390}/I_{440}, I_{390}/I_{460}, I_{380}/I_{500}, I_{390}/I_{500}, I_{440}/I_{500}, I_{450}/I_{500}, I_{460}/I_{500}, I_{470}/I_{500}, and I_{480}/I_{500}. Temporal parameters used for the discriminant function analysis were also selected from the wavelengths mentioned: τ_{370}, τ_{380}, τ_{390}, τ_{440}, τ_{460}, τ_{480}, τ_{450}, τ_{470}, τ_{500}, $\tau_{370:10\%}$, $\tau_{380:10\%}$, $\tau_{390:10\%}$, $\tau_{440:10\%}$, $\tau_{480:10\%}$, $\tau_{460:10\%}$, $\tau_{450:10\%}$, $\tau_{470:10\%}$, and $\tau_{500:10\%}$.

The discriminant functions and classification accuracy were determined for three cases: (1) predictor variables selected from only spectral features, (2) predictor variables selected from only temporal features, and (3) predictor variables selected from both spectral and time-resolved features. The

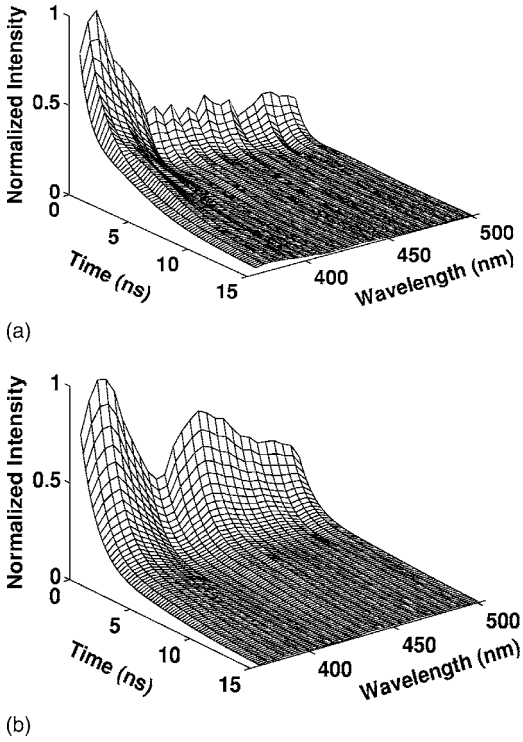

Fig. 2 Representative time-resolved fluorescence emission of (a) meningioma and (b) dura mater.

linear discriminant functions are a linear combination of the independent variables (features), so that the function coefficients perform a linear transformation from the original feature space into an optimal (lower-dimensional) space that provides maximum discrimination. A "leave-one-out" method was used to create the test/training set. This method employs all sets of spectroscopic data except one, as the training set, and then the excluded set is used as the test set.[18] The process is repeated until all data sets are tested. Thus, the left out data set is not a subset of the training set. This approach avoids splitting the available sample set into training and test sets, while maintaining independence between them. The procedure utilizes all available samples more efficiently, and produces a conservative error estimate. The classification accuracy was determined by computing the specificity and sensitivity as follows: sensitivity=true positive predictions/total positive cases; specificity=true negative predictions/total negative cases. The overall classification accuracy =total number of samples correctly classified/total number of samples. Linear discriminant analysis was performed with the software package SPSS® (SPSS Inc.).

3 Results

3.1 *Histology*

Tumors were classified using the World Health Organization (WHO) criteria.[19] Of the total of 97 sites that underwent spectroscopic analysis, 75 were histologically classified as a low-grade meningioma (WHO grade I), 17 as normal dura, and 5 as normal cortex. Most meningiomas, regardless of subtype, demonstrate some fibrous tissue component whether fibrosis, entrapped dura, or fibroblast-like meningioma tumor cells.

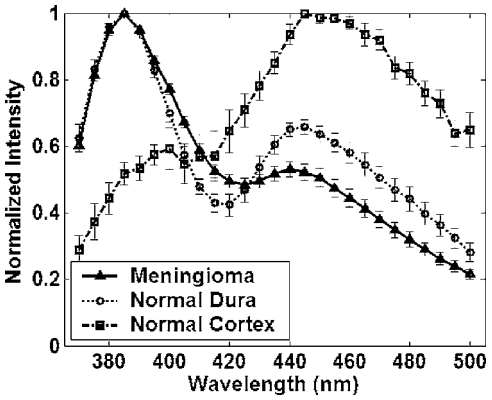

Fig. 3 Normalized integrated fluorescence emission spectra of meningioma, dura mater, and normal cerebral cortex. Results are presented as mean±standard error of the data from each independent measurement.

The extent of extracellular fibrosis or sclerosis ranged from approximately 5% of visualized surface area to approximately 80%. Most meningiomas had a few psammoma bodies focally. A few cases had no psammoma bodies. Two cases demonstrated numerous psammoma bodies. Normal dura samples demonstrate dense fibrous tissue without evidence of tumor. The brain tissue demonstrates layered neurons indicative of cerebral cortex also without evidence of tumor.

3.2 *Time-Integrated and Time-Resolved Fluorescence*

3.2.1 *Meningioma*

The time-resolved fluorescence emission of meningioma samples showed a relatively narrow broadband emission characterized by a well-defined peak at a 385- to 390-nm wavelength [Figs. 2(a) and 3] lasting for more than 15 ns. The fluorescence intensity decay [Figs. 4(a) and 4(b)] was found wavelength-dependent with longer time-decay values in the region of peak fluorescence ($\tau_{390}=2.04\pm0.72$ ns; $\tau_{390:10\%}=8.0\pm1.84$ ns) when compared with the red-shifted wavelengths ($\tau_{460}=1.2\pm0.46$ ns; $\tau_{460:10\%}=5.1\pm1.8$ ns).

3.2.2 *Dura mater*

Typical time-resolved emission spectrum of dura mater is depicted in Fig. 2(b). The emission spectrum (Fig. 3) was characterized by a broad wavelength band with two peaks emission. The main peak is centered at about 385 to 390 nm, the second at about 440 nm. The valley that modulates the spectrum of emission at about 415 nm indicates hemoglobin absorption.[6] The fluorescence lifetime was found slightly longer in the region of main peak emission ($\tau_{390}=1.7\pm0.52$ ns) when compared with the red-shifted wavelengths ($\tau_{460}=1.4\pm0.36$ ns) [Fig. 4(a)]. However, no significant change of the time-dependent parameter, $\tau_{\lambda:10\%}$ values as a function of wavelength was observed. These values were centered at about 5.7 ns along the entire emission spectra [Fig. 4(b)].

3.2.3 *Cerebral cortex*

The normal cortex was characterized by a broad fluorescence emission spectrum (Fig. 3) with well-defined peak between

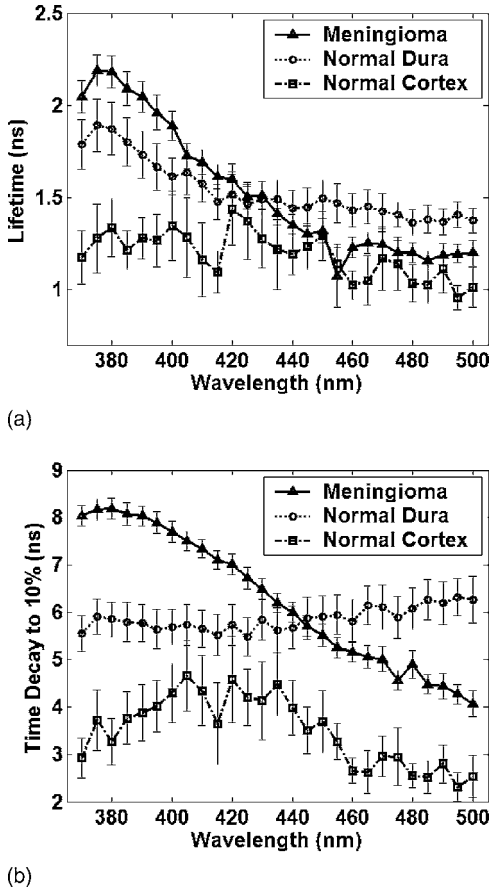

Fig. 4 Time-dependent parameters of meningioma, dura mater, and normal cerebral cortex: (a) average lifetime τ_λ and (b) time-decay to 10% $\tau_{\lambda 10\%}$. Results are presented as mean±standard error of the data from each independent measurement.

440 and 460 nm wavelength. The attenuation of fluorescence intensity at about 415 nm corresponds to the hemoglobin absorption band.[5,6] Across the entire spectrum, the fluorescence emission was short lasting with an average lifetime [Fig. 4(a)] mainly below 1.5 ns (τ_{390}=1.2±0.1 ns; τ_{460}=1.0±0.07 ns) and a decay of the intensity to 10% of its maximum [Fig. 4(b)] in less than 4 ns ($\tau_{390:10\%}$=3.8±0.6 ns; $\tau_{460:10\%}$ =2.6±0.2 ns).

3.2.4 *Statistical analysis and tissues comparison*

In the 385- to 390-nm wavelength region (Fig. 3) meningioma (I_{390}/I_{460}=2.5±1.5) and normal dura matter (I_{390}/I_{460} =1.54±0.3) showed a strong intensity emission when compared with cortex (I_{390}/I_{460}=0.44±0.1). Within this wavelength range, meningioma ($\tau_{460:10}$=5.1±1.8) showed time-decay parameters values similar with dura ($\tau_{460:10}$ =5.8±1.85) but larger than cortex ($\tau_{460:10}$=2.65±0.59) [Fig. 4(a)]. At wavelengths above 430 nm, meningioma exhibited significant lower fluorescence intensity when compared normal tissue, both dura and cortex (Fig. 3). Within this wavelength range, meningioma showed time-decay parameters values similar with dura [Fig. 4(a)] but larger than cortex. The lifetime reproducibility for the five consecutive measurements

Table 1 Classification accuracy (sensitivity and specificity values).

		Meningioma N=75	Normal Dura N=17	Normal Cortex N=5
Spectral values only	Sensitivity	61%	65%	100%
	Specificity	73%	66%	98%
Time-resolved values only	Sensitivity	84%	77%	100%
	Specificity	100%	91%	90%
Spectral+ time-resolved values	Sensitivity	89%	100%	100%
	Specificity	100%	91%	99%

Total number of sites: 97; Meningioma

acquired at 390 nm was within 1 to 11% of the mean value (median value 4.9%), whereas for 460 nm was within 1.5 to 7% (median of 2.1%).

3.2.5 *Discriminant analysis and classification*

The classification accuracy (sensitivity and specificity values) for the discrimination of the meningioma from normal dura and cortex is summarized in Table 1. When only spectral parameters were used as input, the stepwise linear discriminant algorithm selected five parameters (I_{480}/I_{370}, I_{440}/I_{370}, I_{460}/I_{370}, I_{380}/I_{370}, I_{390}/I_{460}). When the classification was performed using only the temporal parameters as input, the discriminant algorithm selected three parameters ($\tau_{370:10\%}$, $\tau_{500:10\%}$, τ_{440}). When both spectral and temporal parameters were used for the analysis, eight significant parameters were selected, I_{390}/I_{460}, I_{380}/I_{370}, I_{390}/I_{370}, and I_{480}/I_{370} from the spectral domain and $\tau_{370:10\%}$, τ_{370}, $\tau_{440:10\%}$, and $\tau_{500:10\%}$ values from the temporal domain. Figure 5 depicts a 2-D scatterplot of two discriminant functions constructed using variables derived from both spectral- and time-resolved domains. It can be observed that function 1 discriminates cortex from dura mater and meningioma, while function 2 enabled discrimina-

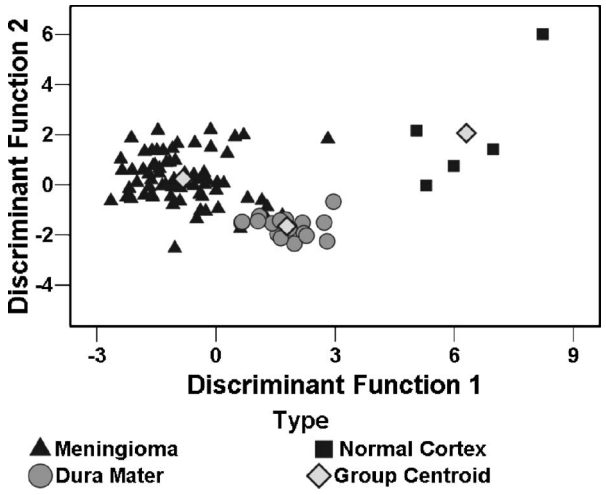

Fig. 5 Results of the linear discriminant function analysis. Scatterplot depicts the discriminant score for the three groups of tissue (meningioma, dura mater, and cerebral cortex).

tion of meningioma from dura mater. In summary, parameters derived from either only spectral features or only temporal features provided means of discrimination between the three tissue groups. However, the overall accuracy of classification improved (91.8% cross-validated set; 92.8% training set) when both spectral and time-resolved features were used for discrimination. In contrast, the overall classification accuracy was lower when either only spectral features (63.9% cross-validated set; 67% training set) or only time-resolved features (83.5% cross-validated set; 85.6% training set) were used as input predictor variables.

4 Discussion

This study is the first to report the application of fluorescence spectroscopy, in particular time-resolved laser-induced fluorescence, to diagnosis of meningiomas. We examined the time-resolved fluorescence emission of meningioma and normal surrounding normal tissue (dura matter and cortex) on 337-nm excitation and determined that meningioma is characterized by unique fluorescence characteristics that allow discrimination of tumor from normal tissue with high sensitivity ($>89\%$) and specificity (100%).

4.1 *Time-Resolved Fluorescence Spectroscopy in Tissue Characterization*

In this study, we employed a time-resolved fluorescence spectroscopy apparatus, enabling the acquisition of fluorescence temporal response across the emission spectrum of tissue specimens, thus both steady state spectra and time-resolved intensity decay can be recovered from a single measurement sequence. We found that combining spectroscopic parameters derived from both spectral and time domains, not only facilitates a better understanding of the kinetics of the biochemical and physiological processes occurring in meningiomas, dura mater, and cortex but also contributed to the improved accuracy of tissue recognition. Although numerous research groups[4,7,12,14] have shown that steady state fluorescence spectroscopy techniques alone are potential tools for diagnosis of tumors, including brain tumors, detection of cancer using only spectral information is subject to several limitations. For example, the relatively broad emission brands of tissue fluorescent components may reduce the capability of this technique to resolve the spectrally overlapping components. Also, the presence of endogenous chromophores (hemoglobin) or changes of excitation/collection geometry can strongly influence the acquired spectral profile. The time-resolved measurement resolves fluorescence intensity decay in terms of lifetimes and thus provides additional information about the underlying fluorescence dynamics. This property has intrinsic advantages, including (1) biomolecules with overlapping fluorescence emission spectra but with different fluorescence decay times can be discriminated; (2) the measurements are sensitive to various parameters of biological microenvironments (including pH and enzymatic activity); and (3) the measurement is independent of fluorescence emission intensity as long as the SNR is commensurable, and consequently independent of the presence of the endogenous chromophores in tissue (hemoglobin) and excitation-collection geometry or optical assembly.[8] These are important features for further *in vivo* studies and intraoperative diagnosis of meningiomas as well as other types of neoplasm.

4.2 *Fluorescence Characteristics and Tissue Recognition*

Two wavelength ranges appeared important for developing diagnostic algorithm for distinguishing meningioma from normal dura and cortex: 370 to 400 nm (the region of main peak emission for meningioma and dura) and 440 to 480 nm (the region of main peak emission for cortex). Note that the dominant narrowband blue-shifted peak emission is a hallmark for meningioma, but it is not always observed in healthy or diseased neuronal tissue including gliomas.[6,7,13,14] The application of multivariate statistical analysis has shown that meningioma, normal dura, and cortex tissues can be differentiated using a relatively limited number of predictor variables (16 in total) from these two spectral ranges. Parameters obtained from both spectral (intensity values) and time-resolved emission contributed to the accuracy of tissue classification. The use of both sets of spectroscopic parameters, spectral and time-resolved, have improved the overall accuracy of meningioma detection (91.8%), compared to the case when only spectral variables were employed (63.9%). Note that the temporal features alone used in discriminant function analysis demonstrate superior ability to classify the tissue than spectral feature alone. Although in this study we used only a small dataset, these results indicate that the time-resolved fluorescence spectroscopy technique is robust enough to enable good discrimination between the three types of tissue investigated in this study. Moreover, the use of time-resolved information enhances the ability to discriminate tumor tissue from the surrounding normal tissue. The classification accuracy may be further improved once the number of samples for dura and normal cortex in the training set increases.

4.3 *Fluorescence of Meningioma, Dura, and Cortex: Interpretation in Terms of Intrinsic Fluorescent Constituents*

The fluorescence intensity time-decay characteristics were found both tissue- and wavelength-dependent. The fluorescence lifetimes τ_λ of meningioma and dura were longer when compared to cortex and decreased significantly with the emission wavelength. These trends suggest that at least two distinct fluorophores are likely to contribute to the fluorescence emission of meningioma and dura. In contrast, the fluorescence emission of normal cortex, characterized by a short-lived emission with nearly constant lifetime values across the emission spectrum, most likely originated from a single fluorophore. Potential sources of fluorescence are outlined in the following.

The fluorescence of connective tissue proteins, in particular collagens, is most likely to dominate the fluorescence emission of dura and meningioma. Several types of collagen and their cross-links are known to absorb light above 300 nm and to exhibit a strong fluorescence emission in 370-nm to 500-nm spectral range.[5,8,20] This assumption is supported by our histopathological analysis, which identified fibrous tissue in both meningioma and dura samples. It is also in agreement with the biochemical and chromatographical analysis of the composition of meningioma and dura reported in other studies

that demonstrated the presence of high concentration of various types of collagen in these tissues.[21] Our results also showed that meningioma and dura were characterized by distinct fluorescence decay dynamic [e.g., dura $\tau_{\lambda:10\%}$ $<$ meningioma $\tau_{\lambda:10\%}$, Fig. 4(b)], albeit having common spectroscopic features such as an intense fluorescence emission in the 370- to 400-nm wavelengths range (peak at $\sim$390 nm) with relatively long-lived fluorescence (τ_{λ} $>$1.5 ns). These differences suggest that fluorescence of meningioma and dura have originated from distinct types of collagens and their cross-links.

For example, studies of fluorophores from collagen-rich fractions of human dura mater using chromatography have demonstrated that two fluorophores are associated with dura fluorescence emission.[22] These are a "P" fluorophore (a pyridinium compound similar to pyridinolines collagen cross-link, peaks excitation/emission: 335/385 nm) and an "M" fluorophore (an age-related fluorophore due to acceleration of collagen browning; peaks excitation/emission: 370/440 nm). Our TR-LIFS measurement on dura mater tissue corroborates with this early study by revealing two peaks emission, one at about 390 and the other at 440 nm. In addition, the change of the fluorescence decay dynamics as a function of wavelength (decrease of τ_{λ} with wavelength, and a near constant $\tau_{\lambda:10\%}$ across the spectrum), as observed in our study, not only confirm the presence of at least two fluorophores in dura matter, but also indicates that these fluorophores are characterized by distinct lifetimes. Our results also suggest that the valley that modulates the spectral emission may not be entirely due to blood presence in tissue or fluorescence reabsorption, as initially assumed.

On the other hand, several immunocytochemical studies have demonstrated the presence in meningioma of collagen I, collagen III, collagen IV, procollagens, laminins, and vimentine.[21] Evidence has also shown that meningioma cells are derived closely from the leptomeningeal arachnoid cells and are "fibrous response" of the leptomeninges to trauma, infection or other pathologies such as tumor infiltration.[21,23,24] The time-resolved spectra of meningiomas in our study, characterized by a relatively narrow-band blue-shifted emission [Fig. 2(a)], closely resemble collagen type I (peak emission 380 nm) and collagen type III (peak 390 nm) fluorescence.[5,8,20] Such trends indicate that these two types of collagen most likely dominated the fluorescence emission of meningioma at the blue-shifted wavelengths.

The short-lived ($<$1.5 ns) fluorescence emission (peak at about 460 nm) found for cortex corresponds to the NAD(P)H fluorescence emission fluorescence. These features are in agreement with previous studies that have reported the spectral[6,7,13,14] as well the lifetime[9] fluorescence emission from cortex. Both forms of NAD(P)H, free in the cytoplasm [low quantum yield of about 2% and lifetimes $<$1 ns (Refs. 25–27)] as well as bound in mitochondria [high quantum yield about fourfold higher than the free form and radiative lifetimes $>$1 ns (Refs. 25–27)] are widely recognized as endogenous fluorophore involved in cellular metabolism,[25,27,28] and probably have originated the fluorescence emission measured from cortex samples. Also, in the red-shifted spectral range, NAD(P)H fluorescence likely contributed to the fluorescence emission of dura mater and meningioma, as depicted by the short lifetimes values determined for these tissues at emission wavelengths above 440 nm.

Further investigations are required for a more complete understanding of the factors of intrinsic fluorophores causing differences in the fluorescence emission properties between meningioma dura, and cortex. Moreover, the metabolic properties of tissue may be different *ex vivo* versus *in vivo*, and these differences can be reflected in tissue fluorescence response.[13] *In vivo* studies will account for such differences and enable direct comparison with the current *ex vivo* studies and better our understanding of how metabolic changes affect the fluorescence data. This study, however, indicated that time-resolved fluorescence spectroscopy represents a potential pathway for nonintrusively gaining insights into the biochemical composition of these tissues.

4.4 *Time-Resolved Fluorescence Spectroscopy Technology: Clinical Perspective*

Neurosurgeons often request frozen section intraoperative tissue specimen analysis from one to many sites during a single surgery for tumor resection. This is generally the case with surgical resection of meningiomas where one to several dural margins are often sent to the neuropathologist for intraoperative diagnosis beyond the initial tumor mass specimen. Rapid identification of neoplastic versus normal tissue using fluorescence-based diagnostics would be a highly beneficial tool for both the surgical pathologist as well as the neurosurgeon.

Moreover, meningiomas are believed to arise from the "arachnoid cap" cells of the arachnoid, although they are intimately associated with the dura mater. Because of their histogenesis, meningiomas develop along any of the external surfaces of the brain as well as within the ventricular system. Common sites of tumor include the convexity, the falx, and the skull base of the anterior, middle, or posterior fossae. Meningiomas occurring "en plaque", or located in anatomically challenging areas such as the petroclival region, present difficulties in achieving complete surgical resections. Thus, a fluorescence spectroscopy may also prove to be valuable intraoperative adjunct for improving completeness of resection in a setting where margins of the neoplastic tissue are indistinct.

In this study, we used the autofluorescent properties of tissue as a diagnostic tool. For a clinical or intraoperative diagnostic of diseased tissue, such an approach has inherent advantages over the use of exogenous fluorophores (molecular probes). The measurement of endogenous fluorescence does not require any systemic or local administration of an external imaging agent, thus problems associated to toxicity and pharmacodynamics/kinetics of the external agent are not encountered. Because diagnosis based on autofluorescent properties of the tissue enables a direct and safe evaluation of the TR-LIFS technique in patients, we have recently developed a clinically compatible TR-LIFS apparatus.[29] Studies are currently being conducted at Cedars-Sinai Medical Center using this apparatus to intraoperatively record the fluorescence of brain tumors including meningioma. These studies will also aid in developing efficient clinical diagnostic procedures that include the detection of tumor margins. Studies have shown that the $1/e$ optical penetration depth for 337-nm excitation

wavelength ranges between 200 and 250 μm depth in a variety of tissues including in brain tissue.[13] Thus, using fiber optic probes with optimal excitation-collection geometry, the presence of tumor at the margins can be detected with relatively high spatial accuracy.

In addition, the analytical methods employed in this study (Laguerre expansion of kernels and linear discriminant analysis) facilitate near real-time data analysis. In a previous study, we demonstrated the ability of the Laguerre expansion of kernels technique for fast (less than 35 ms per wavelength) deconvolution of the fluorescence impulse function and analysis of biological systems.[17] This method enables a direct recovery of the intrinsic properties of a dynamic system from the experimental input-output data.[30] The discriminant function analysis, also, has been explored for automated classification of ^{1}H magnetic rotation spectroscopy (MRS) spectra from brain tumors.[18] A fast real-time classification algorithm can be developed by assigning a discriminant score for different types of tissues. This discriminant score can then be compared with the acquired fluorescence from the unknown tissue so as to classify the tissue in real time. The accuracy of classification by linear discriminant analysis can be increased by continuously acquiring sample for training. Such a combination of analytical methods can aid the neurosurgeon with a real-time optical biopsy of tissue.

Furthermore, our current time-resolved fluorescence spectroscopic system has a potential to be integrated with the current stereotactic-image-guided surgery apparatus; thus, it can provide the surgeon with the diagnostic map of the tissue in view. This particular feature would not only enhance the surgeon's ability to ensure complete resection of various tumors, but may also help in future advances such as robotic surgery where the surgeon can access additional information about the tumor beyond just the visual image.

5 Conclusion

In summary, accurate detection of neoplastic versus normal tissue and demarcation of tumor during neurosurgical interventions play a crucial role in neuropathologic/neurosurgical teamwork. The ability of the neuropathologist to quickly identify the nature of tissue specimens may lead to shortened surgical time and potentially enable better decision making by the surgical team secondary to rapid results from an "optical biopsy." Our findings establish the feasibility of using time-resolved fluorescence spectroscopy as a tool for the identification of meningiomas. Furthermore, time-resolved fluorescence spectroscopy represents a potential tool to aid in a more complete resection of a tumor, which in turn can reduce the recurrence rate and improve survival in patients diagnosed with meningioma. Taking advantage of the tissue autofluorescence, the technique described in this paper facilitates a direct and rapid investigation of diseased tissue and enables further development of real-time diagnostic tools for guiding surgical resection of brain tumors. Moreover, this technique uses fiber optic probes that enable remote investigations. These probes can be readily integrated into the existing surgical neuronavigations systems, thus leading to improved diagnostic capabilities of such systems.

Acknowledgments

This work was supported in part by the Whitaker Foundation (RG-01-0346, PI: L. Marcu). The authors thank Dr. Qiyin Fang, Dr. Javier Jo, and Dr. Thanassis Papaioannou for help with experimental and analytical work.

References

1. I. R. Whittle, C. Smith, P. Navoo, and D. Collie, "Meningiomas," *Lancet* **363**(9420), 1535–1543 (2004).
2. M. S. Greenburg, *Handbook of Neurosurgery*, p. 440, Theime Publishing, New York (2001).
3. L. M. DeAngelis, "Brain tumors," *N. Engl. J. Med.* **344**(2), 114–123 (2001).
4. G. A. Wagnieres, W. M. Star, and B. C. Wilson, "*In vivo* fluorescence spectroscopy and imaging for oncological applications," *Photochem. Photobiol.* **68**(5), 603–632 (1998).
5. R. Richards-Kortum and E. Sevick-Muraca, "Quantitative optical spectroscopy for tissue diagnosis," *Annu. Rev. Phys. Chem.* **47**, 555–606 (1996).
6. W. C. Lin, S. A. Toms, M. Motamedi, E. D. Jansen, and A. Mahadevan-Jansen, "Brain tumor demarcation using optical spectroscopy; an *in vitro* study," *J. Biomed. Opt.* **5**(2), 214–220 (2000).
7. W. C. Lin, S. A. Toms, M. Johnson, E. D. Jansen, and A. Mahadevan-Jansen, "*In vivo* brain tumor demarcation using optical spectroscopy," *Photochem. Photobiol.* **73**(4), 396–402 (2001).
8. L. Marcu, M. C. Fishbein, J. M. Maarek, and W. S. Grundfest, "Discrimination of human coronary artery atherosclerotic lipid-rich lesions by time-resolved laser-induced fluorescence spectroscopy," *Arterioscler., Thromb., Vasc. Biol.* **21**(7), 1244–1250 (2001).
9. L. Marcu, J. A. Javier, P. Butte, W. H. Yong, B. Pikul, K. L. Black, and R. C. Thompson, "Fluorescence lifetime spectroscopy of glioma multiforme," *Photochem. Photobiol.* **80**(1), 98–103 (2004).
10. J. R. Lakowicz, *Principles of Fluorescence Spectroscopy*, 2nd ed., Kluwer Academic/Plenum, New York (1999).
11. R. Cubeddu, D. Comelli, C. D'Andrea, P. Taroni, and G. Valentini, "Time-resolved fluorescence imaging in biology and medicine," *J. Phys. D* **35**(9), R61–R76 (2002).
12. W. S. Poon, K. T. Schomacker, T. F. Deutsch, and R. L. Martuza, "Laser-induced fluorescence: experimental intraoperative delineation of tumor resection margins," *J. Neurosurg.* **76**(4), 679–686 (1992).
13. A. C. Croce, S. Fiorani, D. Locatelli, R. Nano, M. Ceroni, F. Tancioni, E. Giombelli, E. Benericetti, and G. Bottiroli, "Diagnostic potential of autofluorescence for an assisted intraoperative delineation of glioblastoma resection margins," *Photochem. Photobiol.* **77**(3), 309–318 (2003).
14. Y. G. Chung, J. A. Schwartz, C. M. Gardner, R. E. Sawaya, and S. L. Jacques, "Diagnostic potential of laser-induced autofluorescence emission in brain tissue," *J. Korean Med. Sci.* **12**(2), 135–142 (1997).
15. L. Marcu, R. C. Thompson, S. Garde, M. Sedrak, K. L. Black, and W. H. Yong, "Time-resolved fluorescence spectroscopy of human brain tumors," *Proc. SPIE* **4136**, 183–187 (2002).
16. T. Papaioannou, N. W. Preyer, Q. Fang, A. Brightwell, M. Carnohan, G. Cottone, R. Ross, L. R. Jones, and L. Marcu, "Effects of fiber-optic probe design and probe-to-target distance on diffuse reflectance measurements of turbid media: an experimental and computational study at 337 nm," *Appl. Opt.* **43**(14), 2846–2860 (2004).
17. J. A. Jo, Q. Fang, T. Papaioannou, and L. Marcu, "Fast model-free deconvolution of fluorescence decay for analysis of biological systems," *J. Biomed. Opt.* **9**(4), 743–752 (2003).
18. A. R. Tate, J. R. Griffiths, I. Martinez-Perez, A. Moreno, I. Barba, M. E. Cabanas, D. Watson, J. Alonso, F. Bartumeus, F. Isamat, I. Ferrer, F. Vila, E. Ferrer, A. Capdevila, and C. Arus, "Towards a method for automated classification of 1H MRS spectra from brain tumours," *NMR Biomed.* **11**(4–5), 177–191 (1998).
19. P. Kleihues and W. K. Cavenee, "World Health Organization classification of tumors," in *Pathology and Genetics of Tumors of Nervous System*, IARC Press, Lyon (2000).
20. L. Marcu, W. S. Grundfest, and M. C. Fishbein, "Time-resolved laser-induced fluorescence spectroscopy for staging atherosclerotic lesions," in *Handbook of Biomedical Fluorescence*, M. A. Mycek and B. Pogue, Eds., pp. 397–430, Marcel Dekker, New York (2003).
21. H. K. Ng and A. T. Wong, "Expression of epithelial and extracellular matrix protein markers in meningiomas," *Histopathology* **22**(2), 113–

125 (1993).
22. D. R. Sell and V. M. Monnier, "Isolation, purification and partial characterization of novel fluorophores from aging human insoluble collagen-rich tissue," *Connect. Tissue Res.* **19**(1), 77–92 (1989).
23. H. Nitta, T. Yamashima, J. Yamashita, and T. Kubota, "An ultrastructural and immunohistochemical study of extracellular matrix in meningiomas," *Histol. Histopathol* **5**(3), 267–274 (1990).
24. S. S. Gill, D. G. Thomas, N. Van Bruggen, D. G. Gadian, C. J. Peden, J. D. Bell, I. J. Cox, D. K. Menon, R. A. Iles, and D. J. Bryant, "Proton MR spectroscopy of intracranial tumours: *in vivo* and *in vitro* studies," *J. Comput. Assist. Tomogr.* **14**(4), 497–504 (1990).
25. H. Schneckenburger and K. Konig, "Fluorescence decay kinetics and imaging of Nad(P)H and Flavins as metabolic indicators," *Opt. Eng.* **31**(7), 1447–1451 (1992).
26. S. F. Verlick, "Fluorescence spectra and polarization of glyceraldehyde-3-phosphate and lactic dehydrogenase coenzyme complexes 1," *J. Biol. Chem.* **233**(6), 1455–1467 (1958).
27. J. E. Aubin, "Autofluorescence of viable cultured mammalian-cells," *J. Histochem. Cytochem.* **27**(1), 36–43 (1979).
28. K. Konig, M. W. Berns, and B. J. Tromberg, "Time-resolved and steady-state fluorescence measurements of beta-nicotinamide adenine dinucleotide-alcohol dehydrogenase complex during UVA exposure," *J. Photochem. Photobiol., B* **37**(1–2), 91–95 (1997).
29. Q. Fang, T. Papaioannou, J. A. Jo, R. Vaitha, K. Shastry, and L. Marcu, "Time-domain laser-induced fluorescence spectroscopy apparatus for clinical diagnostics," *Rev. Sci. Instrum.* **75**(1), 151–162 (2004).
30. V. Z. Marmarelis, "Identification of nonlinear biological systems using Laguerre expansions of kernels," *Ann. Biomed. Eng.* **21**(6), 573–589 (1993).